Estimating the contribution of Galactic sources to the diffuse neutrino flux

Luis A. Anchordoqui,[1] Haim Goldberg,[2] Thomas C. Paul,[1,2] Luiz H. M. da Silva,[3] and Brian J. Vlcek[4]

[1]*Department of Physics and Astronomy, Lehman College, City University of New York, New York, New York 10468, USA*

[2]*Department of Physics, Northeastern University, Boston, Massachuset 02115, USA*

[3]*Department of Physics, University of Wisconsin-Milwaukee, Milwaukee, Wisconsin 53201, USA*

[4]*Space and Astroparticle Group, Universidad de Alcalá, Alcalá de Henares E-28871, Spain*

(Received 3 October 2014; revised manuscript received 18 November 2014; published 23 December 2014)

Motivated by recent IceCube observations we reexamine the idea that microquasars are high energy neutrino emitters. By stretching to the maximum the parameters of the Fermi engine we show that the nearby high-mass x-ray binary LS 5039 could accelerate protons up to above about 20 PeV. These highly relativistic protons could subsequently interact with the plasma producing neutrinos up to the maximum observed energies. After that we adopt the spatial density distribution of high-mass x-ray binaries obtained from the deep INTEGRAL Galactic plane survey, and we assume LS 5039 typifies the microquasar population to demonstrate that these powerful compact sources could provide a dominant contribution to the diffuse neutrino flux recently observed by IceCube.

DOI: 10.1103/PhysRevD.90.123010 PACS numbers: 98.70.Sa, 95.85.Ry

I. INTRODUCTION

The IceCube Collaboration has quite recently reported the discovery of extraterrestrial neutrinos, including three events with well-measured energies around 1 PeV, but notably no events have been observed above about 2 PeV [1]. At $E_\nu = 6.3$ PeV, one expects to observe a dramatic increase in the event rate for $\bar{\nu}_e$ in ice due to the "Glashow resonance" in which the $\bar{\nu}_e e^- \to W^- \to$ shower greatly increases the interaction cross section [2]. Indeed, the effective detection area near this resonance becomes about 12 times larger than it is off-peak value [3]. However, under the assumption of democratic flavor ratios, only $1/6$ of the total flux is subject to this enhancement. Integrating the effective area for neutrino detection from 2 to 10 PeV, we arrive at a factor of 40 increase (in the energy bin centered at the Glashow resonance) compared to the IceCube sensitivity in the energy bin centered at 1 PeV. This allows one to constrain the hypothesis that the neutrino spectrum follows an unbroken power law. Under the hypothesis of an unbroken power law $\propto E_\nu^{-\alpha}$, the effective area between 2 and 10 PeV together with the three observed neutrinos at ~ 1 PeV lead to an expectation of a flux which obeys $3 \times 40 \times 6.3^{-\alpha} \simeq 3 \times 6.3^{2-\alpha}$. For zero events observed (and none expected from background), Poisson statistics implies that fluxes predicting more than 1.29 events are outside the 68.27% C.L. [4]. Consistency within $1\,\sigma$ then requires $\alpha \geq 2.5$ for energies above about 2 PeV. The event rate derived "professionally" [5] differs by a tiny factor from our back-of-the-envelope estimate. If we assume canonical Fermi shock acceleration dominates below this energy, we would then require a break with a magnitude of roughly $\Delta\alpha = 0.5$.

We note in passing that the strong suppression observed in the ultrahigh energy cosmic ray (UHECR) spectrum ($\propto E^{-\gamma}$) at $E \sim 40$ EeV corresponds to a spectral index change from $\gamma \sim 2.6$ to $\gamma \sim 4.3$, or $\Delta\gamma \sim 1.7$ [6]. This suppression may be due to interactions of UHECRs *en route* to Earth, or it may represent a natural acceleration end point. Indeed, composition data from the Pierre Auger Observatory tend to favor the latter scenario, or possibly a combination of the two effects [7]. If the strong UHECR spectrum does indeed reflect an acceleration end point, it appears that the smaller cutoff of the energy spectrum for neutrinos could also plausibly be attributed to such an effect. Hereafter we assume the spectral break does in fact represent an acceleration end point [8].

Given the overall isotropy of the observed ν arrival directions and the fact that one of the three highest-energy events arrives from outside the Galactic plane, one might suspect an extragalactic origin for the extraterrestrial neutrinos. If the neutrino sources are extragalactic, the γ rays expected to accompany the ν's saturate the γ flux observed by the Fermi satellite for a neutrino spectrum with $\alpha \approx 2.15$ [9]. The statistical analysis sketched above, taken together with the constraint on the spectral index derived from Fermi measurements, points to a spectral cutoff, which precludes a rate increase near the Glashow resonance.

Several explanations have been proposed to explain the origin of IceCube's events [10]. Interestingly, *a priori* predictions for the diffuse ν flux from Fanaroff-Riley I radiogalaxies [11] and starbursts [12] provide a suitable α and normalization for the ν flux while simultaneously retaining consistency with a cutoff at $E_\nu \sim 3$ PeV [13]. Other potential sources that can partially accommodate IceCube data include gamma-ray bursts [14], clusters of galaxies [15] (see, however, Ref. [16]), and active galactic nuclei [17]. However, the identification of extragalactic neutrino point sources from a quasidiffuse flux is

challenging due to the (large) atmospheric neutrino background [18].

On the basis of existing data, a significant contribution from Galactic sources cannot yet be excluded [19,20]. Searches for multiple correlations with the Galactic plane have been recently reported by the IceCube Collaboration [1]. When letting the width of the plane float freely, the best fit corresponds to $\pm 7.5°$ with a posttrial chance probability of 2.8%, while a fixed width of $\pm 2.5°$ yields a p-value of 24%. In particular, some of the events seem to cluster near the Galactic center [21], which has been whimsically described as a neutrino lighthouse [22]. Indeed, a particularly compelling source of some of these neutrinos could be LS 5039 [1]. Figure 1 contains a display of the shower and track events reported by the IceCube Collaboration [1]. Using these data, the collaboration conducted a point source search using an unbinned maximum likelihood method described in Ref. [23]. For both the clustering and point source search, the number of estimated signal events, x_s, is left as a free parameter, and the maximum of the likelihood is found at each location. For the point source search, the most significant source is the binary system LS 5039, with a value of $x_s = 4.9$, and a corresponding p-value of 0.002. Of course there are many sources in the sky; whether this one turns out to be a good candidate, time will tell.

In summary, though the clustering is not statistically significant, one cannot rule out a Galactic origin for some of these events. Motivated by this fact, we perform a generalized calculation of the flux expected from various source distributions, taking account of the location of the Earth in the Galaxy. In particular, we reduce the problem to two specific parameters, the distance to the nearest source and the overall population density. LS 5039 has been discussed in the literature as potential high-energy neutrino emitter [24]. We consider this source as specific example and assume it typifies the population of Galactic microquasars (μQSOs).[1] We generalized the argument such that it can be applied to various source populations. First we bracket the realm of plausibility and consider a uniform distribution and an exponential distribution peaked at the Galactic center. For illustrative purposes, we consider several conceivable different distances to the nearest source. After that we turn our attention to the interesting possibility of μQSOs for which the overall distribution of surface density in the Galaxy has a peak at galactocentric radii 5–8 kpc [27,28].

The layout of the paper is as follows. In Sec. II we revisit the model presented in Ref. [24] in order to better estimate the expected neutrino flux, especially in the PeV region. In Sec. III we compare the properties of LS 5039 with other

[1] μQSOs are a subclass of x-ray binary systems that produce collimated outflows observed as nonthermal radio structures [25]. This particular morphology probably originates in relativistic jets launched from the inner parts of accretion disks around stellar mass black holes or neutron stars [26].

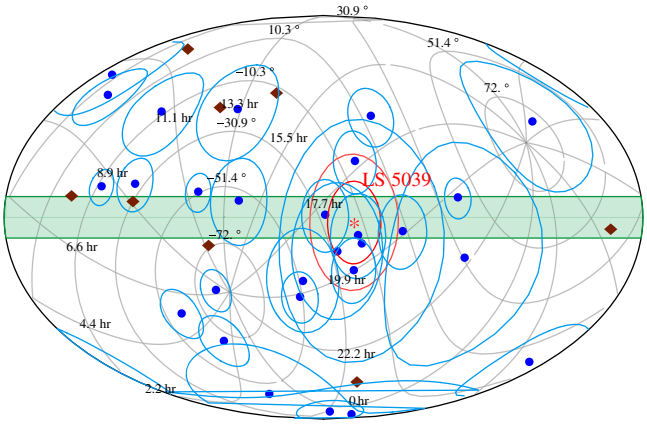

FIG. 1 (color online). The 27 shower events (circles) and 8 track events (diamonds) reported by the IceCube Collaboration in equatorial coordinates. The asterisk indicates the location of LS 5039, and the circular contours centered at this position correspond to radii of 15° and 25°. These contours are designed to help the reader understand how much weight each point contributes to likelihood. The shaded band delimits the Galactic plane.

Galactic microquasars, showing that LS 5039 provides a reasonable lower bound on the power of this type of source. In Sec. IV we estimate the contribution of Galactic sources to the overall diffuse neutrino flux on the assumption that LS 5039 typifies the population. By comparing this estimate with IceCube data, we find the minimum neutrino production efficiency required to dominate the spectrum. In Sec. V we employ constraints from γ-ray observations to bolster our hypothesis. We also address the relevance of our previous finding [20] that a spectral index of 2.3 is consistent with the most recent IceCube spectral shape as well as current bounds on cosmic ray anisotropy. Our conclusions are collected in Sec. VI.

II. ICECUBE NEUTRINOS AS THE SMOKING ICE OF LS 5039 ENGINE

LS 5039 is a high-mass x-ray binary (HMXB) system that displays nonthermal persistent and variable emission from radio frequencies to high-energy (HE), $E_\gamma > 100$ MeV and very-high-energy (VHE), $E_\gamma > 100$ GeV, gamma rays. The system contains a bright ON6.5 V((f)) star [29,30] and a compact object of unknown nature. This degenerate companion has a mass between 1.4 and 5 $M_\odot$ [31]. The orbit of the system has a period of 3.9 days and an eccentricity around 0.35 [31–33]. The distance to the source has recently been updated to 2.9 ± 0.8 kpc [34]. At the apastron the orbital separation of the binary system is 2.9×10^{12} cm and becomes 1.4×10^{12} cm at periastron [31]. Variability consistent with the orbital period in the energy range 100 MeV $\lesssim E_\gamma \lesssim$ 300 GeV was detected by Fermi [35]. The system is also a TeV emitter, with persistent, variable, and periodic emission, as detected by

H.E.S.S. [36,37]. The overall luminosity in the frequency band keV $\lesssim E_\gamma \lesssim$ GeV is $L \sim 10^{35}$ erg s^{-1} [38].

Whether the HE/VHE gamma rays are a of hadronic or leptonic origin is a key issue related to the origin of Galactic cosmic rays. In all gamma-ray binaries, the nature of the compact object is fundamental for understanding the physical processes involved in the particle acceleration that is responsible for the multiwavelength emission. If the compact object were a black hole, the accelerated particles would be powered by accretion and produced in the jets of a μQSO. On the other hand, if the compact object were a young nonaccreting pulsar, the particle acceleration would be produced in the shock between the relativistic wind of the pulsar and the stellar wind of the massive companion star. The detection of elongated asymmetric emission in high-resolution radio images was interpreted as mildly relativistic ejections from a μQSO jet and prompted its identification with an EGRET gamma-ray source [38,39]. However, recent Very Long Baseline Array observations [40] show morphological changes on short time scales that might be consistent with a pulsar binary scenario [41–43]. On the other hand, no short-period pulsations were observed either in radio [44] or x rays [45] definitively demonstrating the compact object to be a pulsar. New IceCube data will clarify this situation, as the only plausible high-energy neutrino emission mechanism requires a compact object powering jets.

Simultaneous production of γ's and ν's generally requires two components: (i) an effective proton accelerator, up to $E \approx 16 E_\nu^{\max}$ and beyond, and (ii) an effective target (converter). The maximum observed neutrino energies then require proton acceleration up to at least $E \gtrsim 20$ PeV. The most likely site for particle acceleration in LS 5039 is the jet, which with a speed $v = 0.2c$ and a half-opening angle $\theta \lesssim 6°$ extends out to 300 milliarcseconds (mas), that is about 10^{16} cm [39]. Within the inner parts of the jet, with a radius $R_{\rm jet} \sim 10^9$ cm, a magnetic field $B \gtrsim 10^5$ G could be sufficient to boost protons up to very high energies. The maximum proton energy is determined by the Hillas condition $r_L \le R_{\rm jet}$, which gives

$$E_{\max} \lesssim 30 \left(\frac{R_{\rm jet}}{10^9\ {\rm cm}}\right)\left(\frac{B}{10^5\ {\rm G}}\right)\ {\rm PeV}, \qquad (1)$$

where r_L is the Larmor radius. A value compatible with this maximum energy has been obtained in an independent calculation [46]. The accelerated protons can interact efficiently with the ambient cold plasma throughout the entire jet. In what follows we assume that the base of the jet is located close to the inner parts of the accretion disk; that is, the jet axis z is taken normal to the orbital plane, as shown in Fig. 2. Here, $z_0 \sim 30 R_{\rm S}$, where

$$R_{\rm S} \simeq 3 \times 10^5 \left(\frac{M_{\rm BH}}{M_\odot}\right)\ {\rm cm} \qquad (2)$$

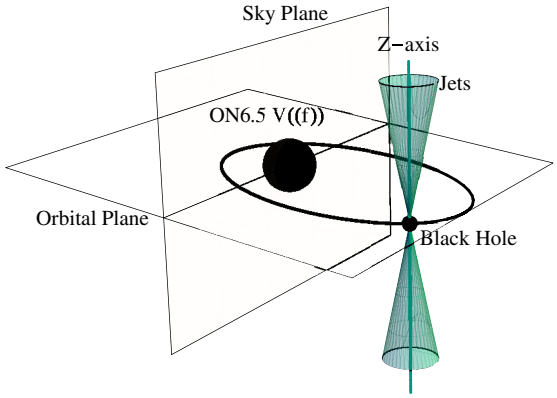

FIG. 2 (color online). Sketch of the binary system.

is the Schwarzschild radius. If the magnetic field drops as $B \propto z^{-1}$, the condition of the confinement of protons in the jet, $r_{\rm L} \le R$ implies $E_{\max} \propto Bz =$ constant, where $R = \theta z$ is the radius of the jet at a distance z. Thus, one may expect acceleration of protons to the same maximum energy $E_{\max}$ over the entire jet region. However, if there is a faster drop of B with z, the protons at some distance z_t from the compact object will start escaping the jet. If this happens within the binary system, i.e., $z_t \le 10^{12}$ cm, protons interacting with the dense wind of the optical star will result in additional γ-ray and neutrino production outside the jet.

If the jet power is dominated by the kinetic energy of bulk motion of cold plasma, the baryon density of the jet $n_{\rm jet}$ can be estimated from the jet power,

$$L_{\rm jet} = \frac{\pi}{2} R_{\rm jet}^2(z) n_{\rm jet}(z) m_p v^3. \qquad (3)$$

The efficiency of γ-ray production in the jet is

$$\rho_\gamma = \frac{L_\gamma}{L_p} = \sigma_{pp} f_\pi \int_{z_0}^{z_t} n_{\rm jet}(z) dz \le 1, \qquad (4)$$

where L_γ is the luminosity of VHE γ rays and L_p is the power of accelerated protons. Here, $\sigma_{pp} \approx 40$ mb is the cross section of inelastic pp interactions, and $f_\pi \approx 0.15$ is the fraction of the energy of the parent proton transferred to a high- energy γ ray [47]. Given the recent estimate of the black hole mass in LS 5039 $M = 3.7^{+1.3}_{-1.0} M_\odot$ [31], we set $z_0 \simeq 3 \times 10^7$ cm. For the profile of the number density, we adopt a power law form $n_{\rm jet} = n_0 (z_0/z)^{-s}$, where $s = 0$ for a cylindrical geometry, $s = 2$ for a conical jet, and $s = 1$ for the intermediate case. Expressing the acceleration power of protons in terms of the total jet power, $L_p = \kappa L_{\rm jet}$, one finds the following requirement for the jet power,

$$L_{\rm jet} \approx 2 \times 10^{37} \frac{L_{\gamma,34}^{1/2} (\nu/0.2c)^{3/2}}{\sqrt{\mathcal{C}(s)\kappa/0.1}}\ {\rm erg\ s^{-1}}, \qquad (5)$$

where $l_{\gamma,34} = L_\gamma/10^{34}$ erg s^{-1} and κ is the acceleration efficiency. The parameter $\mathcal{C}(s)$ characterizes the geometry/density profile of the jet: for $s = 0, 1, 2$, we find $\mathcal{C}(s) = z_t/z_0, \ln(z_t/z_0)$, and 1, respectively. The cylindrical geometry provides the highest efficiency of γ-ray production. However, since $L_\gamma \lesssim 1/30 L_{\rm jet}$ (assuming $\approx 10\%$ efficiency of proton acceleration, and taking into account that the fraction of energy of protons converted to γ rays cannot exceed 30%), the γ-ray production cannot be extended beyond $z_t \sim 10^4 z_0 \sim 3 \times 10^{11}$ cm. The conical geometry corresponds to the minimum efficiency of γ-ray production and thus the largest kinetic power of the jet. In this case the bulk of γ rays are produced not far from the base. For $s = 1$, γ rays are produced in equal amounts per decade of length of the jet, until the jet terminates.

If γ rays are indeed produced in pp interactions, one would expect production of high-energy neutrinos at a rate close to the γ-ray production rate. However, since γ rays are subject to energy-dependent absorption, both the energy spectrum and the absolute flux of neutrinos,

$$\phi_\nu(E_\nu) \simeq 2\phi_\gamma(E_\gamma)\exp[\tau(E_\gamma)], \tag{6}$$

could be quite different from that of the detected γ rays, where $E_\nu \simeq E_\gamma/2$. The optical depth $\tau(E)$ depends significantly on the location of the γ-ray production region and therefore varies with time if this region occupies a small volume of the binary system. This may lead to time modulation of the energy spectrum and the absolute flux of TeV radiation with the orbital period [48]. Moreover, the $\gamma\gamma$ interactions generally cannot be reduced to a simple effect of absorption. In fact, these interactions initiate high-energy electron-photon cascades, driven by inverse Compton scattering and $\gamma\gamma$ pair production. The cascades significantly increase the transparency of the source. The spectra of γ rays formed during the cascade development significantly differ from the spectrum of γ rays that suffer only absorption.

To model the electromagnetic cascade developed in the plasma, we adopt the method described in Ref. [49]. In our calculations we include the three dominant processes driving the cooling of the electromagnetic cascade: photon-photon pair production, inverse Compton scattering, and synchrotron radiation from electrons. Because of the orbital motion, both the absolute density and the angular distribution of the thermal radiation of the star relative to the position of the compact object vary with time. We take into account the effect induced by the anisotropic (time-dependent) distribution of the target photons on the Compton scattering and pair-production processes [50]. We normalize the cascade spectrum of photons to the flux reported by the H.E.S.S. Collaboration in the TeV energy range [36,37]. Interestingly, if pion production is mostly dominated by collisions close to the base of the jet (i.e., $z \lesssim 10^8$ cm), then the resulting flux of γ rays can marginally accommodate observations in the GeV range

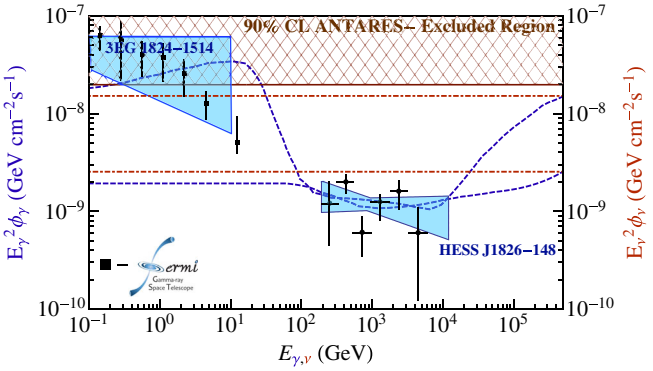

FIG. 3 (color online). The dashed curves represent the time averaged γ-ray spectra of LS 5039 after cascading in the anisotropic radiation field of the normal companion star. The curves are normalized to reproduce the observed γ-ray flux by H.E.S.S. in the TeV range [36,37]. If pions are produced near the base of the jet, the γ's produced through π^0 decay can trigger cascades in the plasma, yielding a photon flux which can marginally accommodate EGRET [51] and Fermi [35] data. The dot-dashed horizontal lines indicate the accompanying neutrino flux. All curves are averaged over the orbital period taking into account data on the geometry of the binary system [31]. The cross-hatched area indicates the 90% upper limit on the flux from LS 5039 reported by the ANTARES Collaboration [53].

[35,51]. However, if pion production takes place well above the base of the jet ($z = 10^{13}$ cm), the flux of GeV photons becomes about an order of magnitude smaller. These two extreme situations, which are shown in Fig. 3, provide an upper and a lower bound on the resulting neutrino flux

$$\phi_\nu(E_\nu) = \zeta E_\nu^{-2}\ \text{GeV}^{-1}\,\text{cm}^{-2}\,\text{s}^{-1}, \tag{7}$$

where $1.8 \times 10^{-9} < \zeta < 1.6 \times 10^{-8}$. The lower value of ζ is in good agreement with the results of Ref. [52].[2] It is notable that, while our results are ultimately derived from demanding consistency between neutrino and photon data, the results in Ref. [52] are derived from assumption on source parameters. For a source distance $d \simeq 3$ kpc, the flux range given in (7) corresponds to an integrated luminosity per decade of energy,

$$\begin{aligned} L_\nu^{\rm LS\,5039} &= 4\pi d^2 \int_{E_1}^{E_2} E_\nu \phi(E_\nu) dE_\nu \\ &= 4\pi \left(\frac{d}{\rm cm}\right)^2 \zeta \ln 10\ \text{GeV}\,\text{s}^{-1}, \end{aligned} \tag{8}$$

in the range $E 7.0 \times 10^{33}\,\text{ergs}^{-1} \lesssim L_\nu^{\rm LS5039} \lesssim 6.4 \times 10^{34}\,\text{ergs}^{-1}$.

[2]The two analyses assume the same fiducial value for κ. Good agreement is achieved by taking the fiducial value for the fraction of the jet kinetic energy which is converted to internal energy of electrons and magnetic fields.

Herein we have assumed the usual Fermi injection spectral index of $\alpha = 2$. The spectral index of γ radiation measured by H.E.S.S. varies depending upon the orbital configuration, reaching a maximum value of 2.53 [36,37]. In the next two sections, we will assume the "traditional" spectral index. In Sec. V we comment on the effect of a steeper spectrum.

Determining whether this analysis can be straightforwardly generalized to all sources in the Galaxy depends on whether neutrino emission from LS 5039 can typify the population of μQSOs. It is this what we now turn to study.

III. GENERALITIES OF THE MICROQUASAR POPULATION IN THE GALAXY

The most recent catalogs show 114 HMXBs [54] and about 130 low-mass x-ray binaries (LMXBs) [55]. The INTEGRAL/IBIS nine-year Galactic plane survey, limited to $|b| < 17°$, contains 82 high-mass and 108 low-mass sources [56]. The sensitivity of this survey is about 10^{-11} erg s^{-1} cm^{-2} in the 17–60 keV energy band, which ensures detection of sources with luminosities $\gtrsim 10^{35}$ erg s^{-1} within half of the Galaxy ($\lesssim$9 kpc from the Sun) and $\gtrsim 5 \times 10^{35}$ erg s^{-1} over the entire Galaxy ($\lesssim$20 kpc from the Sun); see Fig. 4. The number of x-ray binaries in the Galaxy brighter than 2×10^{34} erg s^{-1} is thought to comprise 325 HMXBs and 380 LMXBs [28]. These estimates may be uncertain by a factor of approximately 2 due to our limited knowledge of the source spatial distribution, rendering them consistent with the observations from the surveys reported above. Taken together this suggests an upper limit of μQSOs in the Galaxy of $\mathcal{O}(100)$ [57].

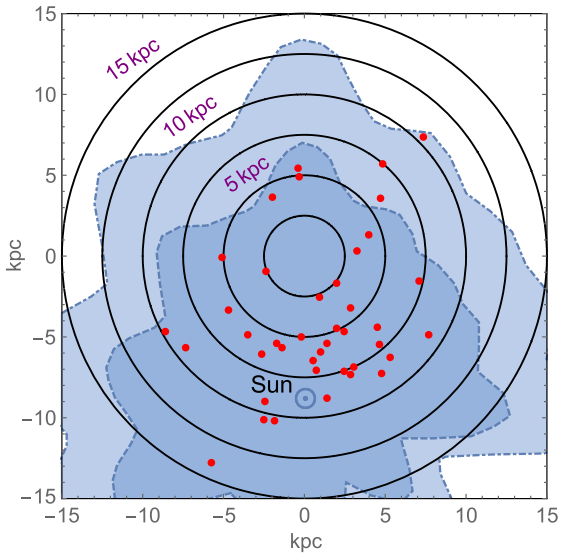

FIG. 4 (color online). Illustrative view of the surface density of HMXBs in the Galaxy. The red points indicate positions of HMXBs. The dot-dashed and dashed curves show the regions of the Galaxy, within which the INTEGRAL Galactic survey detects all sources with luminosities $> 10^{35.5}$ erg s^{-1} and $> 10^{35}$ erg s^{-1}.

About 20 μQSOs have been discovered so far. An illustrative sample can be found in Table I. Note that the estimated jet luminosity of LS 5039 is relatively low, implying that we can in principle use this source to estimate a lower bound on the neutrino production efficiency required to be consistent with observation. Note also that the only source with $L_{\rm jet}$ less than that for LS 5039 has been observed in bursting and quiescent states. In Table I we quote the quiescent value which is about a factor of 2 lower than for the case of bursting state [58].

A comparison among all IceCube events and the Galactic μQSO population is shown in Fig. 5. Not surprisingly given the size of the localization error, the two PeV neutrino events with arrival direction consistent with the Galactic plane can be associated with μQSOs within $1\,\sigma$ uncertainties.

It appears that the impulse from supernovae explosions can eject a system from its original position in the disk into the halo. In fact a number of μQSOs have been observed with very high velocities. For instance, XTE J1118-480 moves at 200 km s^{-1} in an eccentric orbit around the Galactic center [63]. Additionally, the position and velocity of Scorpius X-1 suggest it is a halo object [64]. Such speedy objects are called runaway μQSOs. LS 5039 qualifies as such a runaway μQSO with a velocity of 150 km s^{-1}. Its computed trajectory suggests it could reach a Galactic latitude of $\sim 12°$. The IceCube analysis search for multiple correlation in the Galactic plane favors latitudes less than about $\pm 7.5°$, which is not inconsistent with the latitude reached by runaway μQSOs.

The next-to-highest-energy neutrino event is not in the Galactic plane. It is also interesting to note that the position of this PeV event is within 10° in the hottest spot of IceCube search [65] for PeV γ-ray sources [66]. If it turns out that PeV photons and neutrinos are generated at the same sites, then observation of coincidences implies these sites must be within the Galaxy, given the short mean free path of PeV photons, which is less than 10 kpc. Conceivably, this could be associated with an as-yet-undiscovered μQSO.

At about 2 kpc from Earth, there is another HMXB system with similar characteristics to LS 5039. LS I + 61 303 has been detected at all frequencies, including TeV and GeV energies [67]. Observations of persistent jetlike features in the radio domain at $\sim$ 100 mas scales prompted a classification of the source as a μQSO [68], but subsequent observations at $\sim$ 1–10 mas scales, covering a whole orbital period, revealed a rotating elongated feature that was interpreted as the interaction between a pulsar wind and the stellar wind [41]. More recently, evidence favoring LS I + 61 303 as the source of a very short x-ray burst led to the analysis of a third alternative: a magnetar binary [69]. This binary system has also been suspected to be a high-energy neutrino emitter [70]. The source has been periodically monitored by the AMANDA and IceCube

TABLE I. Properties of μQSOs in the Galaxy.

Classification	Name	Position (J2000.0)	Distance (kpc)	$L_{\rm jet}$ (erg/s)	Reference
HMXB	LS I + 61 303	$(02^{\rm h}40^{\rm m}31.70^{\rm s}, +61°13'45.6'')$	2	5.69×10^{36}	[52]
HMXB	CI Cam	$(04^{\rm h}19^{\rm m}42.20^{\rm s}, +55°59'58.0'')$	1	5.66×10^{37}	[52]
LMXB	GRO J0422 + 32	$(04^{\rm h}21^{\rm m}42.70^{\rm s}, +32°54'27.0'')$	3	4.35×10^{37}	[52]
LMXB	XTE J1118 + 480	$(11^{\rm h}18^{\rm m}10.79^{\rm s}, +48°02'12.3'')$	1.9	3.49×10^{37}	[52]
LMXB	GS 1354-64	$(13^{\rm h}58^{\rm m}09.70^{\rm s}, -64°44'05.0'')$	10	3.62×10^{37}	[52]
LMXB	Circinus X-1	$(15^{\rm h}20^{\rm m}40.84^{\rm s}, -57°10'00.5'')$	10	7.61×10^{38}	[52]
LMXB	XTE J1550-564	$(15^{\rm h}50^{\rm m}58.67^{\rm s}, -56°28'35.3'')$	2.5	2.01×10^{38}	[52]
LMXB	Scorpius X-1	$(16^{\rm h}19^{\rm m}55.09^{\rm s}, -15°38'24.9'')$	2.8	1.04×10^{38}	[52]
LMXB	GRO J1655-40	$(16^{\rm h}54^{\rm m}00.16^{\rm s}, -39°50'44.7'')$	3.1	1.6×10^{40}	[52]
LMXB	GX 339-4	$(17^{\rm h}02^{\rm m}49.40^{\rm s}, -48°47'23.3'')$	8	3.86×10^{38}	[52,59]
LMXB	1E 1740.7-2942	$(17^{\rm h}43^{\rm m}54.82^{\rm s}, -29°44'42.8'')$	8.5	$10^{36} - 10^{37}$	[60]
LMXB	XTE J1748-288	$(17^{\rm h}48^{\rm m}05.06^{\rm s}, -28°28'25.8'')$	8	1.84×10^{39}	[52]
LMXB	GRS 1758-258	$(18^{\rm h}01^{\rm m}12.40^{\rm s}, -25°44'36.1'')$	8.5	$10^{36} - 10^{37}$	[61]
HMXB	V4641 Sgr	$(18^{\rm h}19^{\rm m}21.63^{\rm s}, -25°24'25.9'')$	9.6	1.17×10^{40}	[52]
HMXB	LS 5039	$(18^{\rm h}26^{\rm m}15.06^{\rm s}, -14°50'54.3'')$	2.9	8.73×10^{36}	[52]
HMXB	SS 433	$(19^{\rm h}11^{\rm m}49.57^{\rm s}, +04°58'57.8'')$	4.8	1.00×10^{39}	[52]
LMXB	GRS 1915+105	$(19^{\rm h}15^{\rm m}11.55^{\rm s}, +10°56'44.8'')$	12.5	2.45×10^{40}	[52]
HMXB	Cygnus X-1	$(19^{\rm h}58^{\rm m}21.68^{\rm s}, +35°12'05.8'')$	2.1	$10^{36} - 10^{37}$	[62]
HMXB	Cygnus X-3	$(20^{\rm h}32^{\rm m}25.77^{\rm s}, +40°57'28.0'')$	10	1.17×10^{39}	[52]

collaborations [71]. The most recent analysis leads to a 90% C.L. upper limit on the neutrino flux at the level $E_\nu^2 \Phi_{90}(E_\nu) = 1.95 \times 10^{-9}\ {\rm GeV\,cm^{-2}\,s^{-1}}$ [72]. This implies that if we were to consider LS 5039 as a standard neutrino source of the μQSO population then γ's and ν's should be produced well above the base of the jet, without γ-ray absorption. For such a case, the predicted neutrino flux is compatible with an independent analysis presented in Ref. [21], which assumes the neutrino cluster arrives from the direction of the Galactic center. Such a flux is also compatible with studies described in Ref. [10], which also postulate a Galactic center origin, but with steeper spectral indices. Finally, we stress that the predicted high-energy neutrino flux that can typify the μQSO population is about an order of magnitude below the 90% upper limit reported by the ANTARES Collaboration [53]; see Fig. 3.

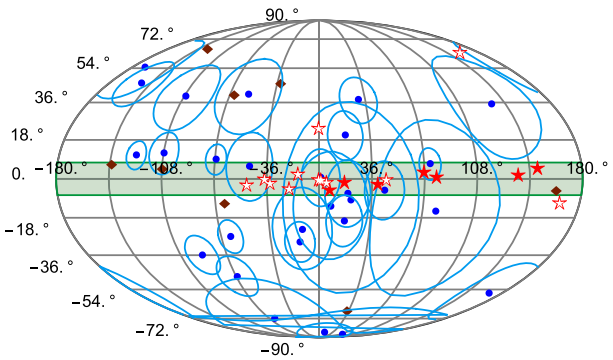

FIG. 5 (color online). Comparison of IceCube event locations [1] with Galactic μQSOs in a Mollweide projection. The 27 shower events are indicated by circles and the 8 track events by diamonds. The solid stars indicate the 7 μQSOs classified as HMXB and the outlined stars the 12 μQSOs classified as LMXB. The shaded band delimits the Galactic plane.

In summary, if we assume the luminosity of LS 5039 truly typifies the power of a μQSO, then we should adopt as fiducial $L_\nu^{\rm LS\,5039} \approx 10^{33}\ {\rm erg\,s^{-1}}$; otherwise we will be inconsistent with the IceCube limit on LS I + 61 303. However, it is important to stress that the value of $L_\nu^{\rm LS\,5039}$ we will adopt to typify the population is very conservative for far away sources, as one can observe in Table II. In closing, we note that though the IceCube bounds are currently the most stringent, ANTARES has the potential to discover exceptionally bright bursting sources in the Southern sky [73].

IV. HIGH-ENERGY NEUTRINOS FROM GALACTIC MICROQUASARS

Galactic μQSOs have long been suspected to be sources of high-energy neutrinos [46]. In this section, we consider the overall contribution of these candidate sources to the diffuse neutrino flux, assuming LS 5039 is the nearest

TABLE II. 90% C.L. upper limits on the squared energy weighted flux of $\nu_\mu + \nu_{\bar\mu}$ in units of $10^{-9}\ {\rm GeV\,cm^{-2}\,s^{-1}}$.

Name	$E_\nu^2 \Phi_{90\%\rm C.L.}^{\rm IceCube}$	$E_\nu^2 \Phi_{90\%\rm C.L.}^{\rm ANTARES}$	Reference
LS I 63 303	1.95	…	[72]
Circinus X-1	…	16.2	[53]
GX 339-4	…	15.0	[53]
LS 5039	…	19.6	[53]
SS 433	0.65	23.2	[53,72]
Cygnus X-3	1.70	…	[72]
Cygnus X-1	2.33	…	[72]

source and typifies the μQSO population. We improve the procedure sketched elsewhere [10], in which the Earth was assumed to be at the edge of the Galactic disk. In our current approach, we place the Earth in its actual position (about 8 kpc from the Galactic center) and perform the requisite integrations numerically. We further enhanced our previous analysis by considering several source distributions. First, we assume the sources are uniformly distributed. Second, we assume the source density decreases exponentially with the distance from the Galactic center. These extremes are likely to bound the true source distribution. Finally, we consider a more realistic distribution to describe the particular case of μQSOs.

The ensuing discussion will be framed in the context of the thin disk approximation. We model the Milky Way as a cylinder of radius $R_G = 15$ kpc and thickness $\delta = 1$ kpc. Consider the situation displayed in Fig. 6 in which the observer O is at the Earth, located at a distance $R = 8.3$ kpc from the center of the Galaxy C. Denote the vector from O to C by $\vec{R}$, from C to the source S_i by $\vec{r}_i'$, and from O to S_i by $\vec{r}_i$; then $\vec{r}_i = \vec{R} + \vec{r}_i{}'$, and so $r_i^2 = R^2 + r_i{}'^2 + 2Rr_i'\cos\theta$. The integrated energy weighted total neutrino flux from the *isotropic* Galactic source distribution with normal incidence at O is

$$4\pi\int_{E_1}^{E_2} E_\nu\Phi(E_\nu)dE_\nu = \frac{1}{4\pi}\sum_i \frac{L_{\nu,i}}{r_i^2} = \frac{1}{4\pi}\sum_i \frac{L_{\nu,i}}{R^2 + 2Rr'\cos\theta + r'^2}, \tag{9}$$

where $L_{\nu,i}$ is the power output of source i and θ is the angle subtended by $\vec{r}_i'$ and $\vec{R}$. Assuming equal power for all sources, $L_{\nu,i} = L_\nu^{\mathrm{LS}\,5039}$, we convert the sum to an integral,

$$4\pi\int_{E_1}^{E_2} E_\nu\Phi(E_\nu)dE_\nu = \frac{L_\nu^{\mathrm{LS}\,5039}}{4\pi}\iint \frac{\sigma(r')r'dr'd\theta}{R^2 + r'^2 + 2Rr'\cos\theta}, \tag{10}$$

where $\sigma(r')$ is the source number density. Any infrared divergence in (10) is avoided by cutting off the integral within the void of radius h as shown in Fig. 6. For the sector of the circle (i) containing the observer, the integral in (10) can be written as

$$\mathcal{I}_1 = \int_{\pi+\phi}^{\pi-\phi} d\theta\int_0^{r_1}\frac{\sigma(r')r'dr'}{R^2 + r'^2 + 2Rr'\cos\theta} + \int_{\pi+\phi}^{\pi-\phi} d\theta\int_{r_2}^{R_G}\frac{\sigma(r')r'dr'}{R^2 + r'^2 + 2Rr'cos\theta}, \tag{11}$$

where $\sin\phi = h/R$. To determine r_1 we use the cosine law, $h^2 = r_1^2 + R^2 - 2Rr_1\cos\beta$,

$$r_1 = R\cos\beta \pm \sqrt{h^2 - R^2\sin^2\beta}, \tag{12}$$

where $\beta = \pi - \theta$. For $\beta = 0$, we must recover $r_1 = R - h$, and so we take the minus sign in (12). The geometry of the problem then allows identification of r_2 as the solution with the positive sign in (12). For the sector of the circle (ii) outside the observer, the integral in (10) becomes

$$\mathcal{I}_2 = \int_0^{R_G}\int_{-\pi+\phi}^{\pi-\phi}\frac{\sigma(r')r'dr'd\theta}{R^2 + r'^2 + 2Rr'\cos\theta}. \tag{13}$$

Putting all this together, for $E_1 \sim 100$ TeV and $E_2 \sim 1$ PeV, the diffuse neutrino flux on Earth is given by

$$E_\nu^2\Phi(E_\nu) = \frac{d^2E_\nu^2\phi_\nu(E_\nu)}{4\pi}(\mathcal{I}_1 + \mathcal{I}_2) = \frac{d^2\zeta}{4\pi}(\mathcal{I}_1 + \mathcal{I}_2) = \frac{L_\nu^{\mathrm{LS}\,5039}}{16\pi^2\ln 10}(\mathcal{I}_1 + \mathcal{I}_2). \tag{14}$$

For 100 TeV $\lesssim E_\nu \lesssim$ 3 PeV, the IceCube Collaboration reports a flux

$$\Phi(E_\nu) = 1.5\times10^{-8}\left(\frac{E_\nu}{100\ \mathrm{TeV}}\right)^{-2.15\pm0.15}(\mathrm{GeV\,cm^2\,s\,sr})^{-1},$$

assuming an isotropic source distribution and democratic flavor ratios [1]. For direct comparison with IceCube data, (14) can be rewritten in standard units using the fiducial value of the source luminosity derived in the previous section,

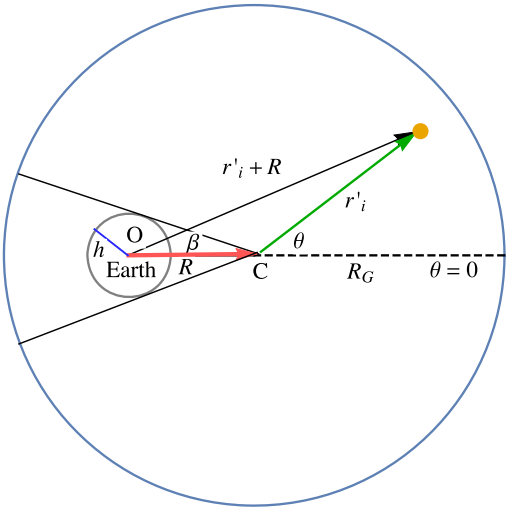

FIG. 6 (color online). Sketch used to arrive at Eqs. (11) and (13). Notice that we take account of the approximate location of the Earth in the Galactic disk. h is a void placed around the Earth to regularize the integration (see the text).

$$E_\nu^2 \Phi(E_\nu) \approx 1.27 \times 10^{-19}\ \mathrm{GeV\,cm^{-2}\,s^{-1}\,sr^{-1}} \frac{\mathcal{I}_1 + \mathcal{I}_2}{\mathrm{kpc}^2}. \tag{15}$$

The integrals $\mathcal{I}_1$ and $\mathcal{I}_2$ have been computed numerically for various void configurations assuming equal power density per unit area of the disk, that is $\sigma_\Theta(r') = N/\pi R_G^2$, where N is the total number of sources. The results are given in Table III. The number of sources required to provide a dominant contribution to IceCube data depends somewhat on the size of the void h. For $h \approx 3$ kpc, about 900 sources are needed to match IceCube observations. This corresponds to a total power in neutrinos of about 6×10^{36} erg s^{-1}. If we assume that these accelerators also produce a hard spectrum of protons with equal energy per logarithmic interval, then the estimate of the total power needed to maintain the steady observed cosmic ray flux is more than 2 orders of magnitude larger [20,74].

In this paper we have advocated a scenario in which a nearby source contributes significantly to the overall flux, rendering it anisotropic. Should this be the case, *the isotropic contribution to the overall flux must be smaller than that derived based on the assumption that all IceCube events contribute to the isotropic flux.* To model the isotropic background of the nearby source scenario, we duplicate the procedure substituting in (10) an exponential distribution of sources which is peaked at the Galactic center, $\sigma_{\rm exp}(r') = n_0 e^{-r'/r_0}$. We normalize the distribution to the total number of sources in the Galaxy, $N = \int_0^{2\pi} d\theta \int_0^{R_G} \sigma_{\rm exp}(r') r' dr'$. Because we have two parameters, we need an additional constraint. We choose to restrict the percentage of the total number of sources beyond the distance $R - h$ to the Galactic edge R_G,

$$P_{R-h} = 2\pi \int_{R-h}^{R_G} n_0 e^{-r'/r_0} r' dr', \tag{16}$$

We choose to take $P_{R-h} = 10\%$. The number of sources required to produce a diffuse neutrino flux at the level reported by the IceCube Collaboration is given in Table IV, for different values of h.

Recent studies [27,28] of persistent HMXBs in the Milky Way, obtained from the deep INTEGRAL Galactic plane survey [56], provide us a new insight into the population of μQSOs. The HMXB surface densities (averaged over corresponding annuli) are given in Table V. It can be seen that the overall distribution of surface density in the Galaxy has a peak at galactocentric radii of 5–8 kpc and that HMXBs tend to avoid the inner 2–4 kpc of the Galaxy [28]. Therefore, it is clear that a simple exponential disk component is not a good description for the radial distribution. In the spirit of Ref. [75], we assumed a source density distribution in the form

$$\sigma_{\mu\rm QSO}(r') = N_0 \exp\left[-\frac{R_0}{r'} - \frac{r'}{R_0}\right], \tag{17}$$

where the first term in the exponential allows for the central density depression. To describe the observed central depression for high-mass x-ray binaries, we take $R_0 = 4$ kpc [28]. This is also supported by a fit to the data in Table V. The number of sources required to produce a diffuse neutrino flux at the level reported by the IceCube Collaboration is given in Table IV, for different values of h. For a void of 1 kpc, which is the distance to the nearest source in Table I (CI Cam), about 500 sources are needed to reproduce IceCube observations.

It is worth commenting on an aspect of this analysis which may seem discrepant at first blush. We find that some 500 μQSOs are required to satisfy energetics requirements, while current catalogs/estimates describe about 100 such known objects. This is not so worrying for the following reasons. First, we have considered only the lower bound on μQSO jet luminosity, which may vary by up to 3 orders of magnitude in the catalog listings (see Table I). In this sense our estimated required number of μQSOs that can plausibly

TABLE III. Results for numerical integration of (11) and (13), assuming various source distributions, and equivalent point source number N. The values listed in the table are in units of kpc^{-2}.

h (kpc)	$(\mathcal{I}_1 + \mathcal{I}_2)_\Theta$	$(\mathcal{I}_1 + \mathcal{I}_2)_{\rm exp}$	$(\mathcal{I}_1 + \mathcal{I}_2)_{\mu\rm QSO}$
1	0.0224 N	0.0211 N	0.0273 N
2	0.0163 N	0.0178 N	0.0193 N
3	0.0127 N	0.0163 N	0.0146 N
4	0.0101 N	0.0154 N	0.0113 N
5	0.0081 N	0.0148 N	0.0088 N

TABLE IV. Number of sources required for each distribution to dominate the neutrino flux reported by the IceCube Collaboration.

h (kpc)	N_Θ	$N_{\rm exp}$	$N_{\mu\rm QSO}$
1	527	560	433
2	724	663	612
3	930	725	809
4	1169	767	1045
5	1458	798	1342

TABLE V. Best-fit parameters of the HMXB spatial density distribution.

r' (kpc)	$N(L > 10^{35}\ \mathrm{erg\,s^{-1}})\mathrm{kpc}^{-2}$
0–2	0.0 ± 0.05(syst)
2–5	$0.11^{+0.05}_{-0.04}$(stat) $\pm$ 0.02(syst)
5–8	$0.13^{+0.04}_{-0.03}$(stat) $\pm$ 0.01(syst)
8–11	$(3.8^{+2.1}_{-1.2}) \times 10^{-2}$(stat) $\pm 6.5 \times 10^{-3}$(syst)
11–14	$(6.2^{+7.2}_{-4.3}) \times 10^{-3}$(stat) $\pm 4.8 \times 10^{-3}$(syst)

explain the IceCube data is a conservative one. Second, when considering the nearby source scenario, we did not reevaluate the background conditions, which would yield a smaller isotropic flux.[3] Again, this is a conservative path. Thus, the analysis presented herein adheres to a "cautious" approach throughout, lessening (or eliminating) concerns about the discrepancy between our estimates of the required number of μQSOs vs the cataloged quantities. We then conclude that μQSOs could provide the dominant contribution to the diffuse neutrino flux recently observed by IceCube.

V. CONSTRAINTS FROM GAMMA RAYS AND BARYONIC COSMIC RAYS

Very recently the IceCube Collaboration has extended their neutrino sensitivity to lower energies [76]. One intriguing result of this new analysis is that the spectral index which best fits the data has steepened from 2.15 ± 0.15 to 2.46 ± 0.12. If one assumes the neutrino spectrum follows a single power law up to about 10 GeV, then the latest data from the Fermi telescope [77] can be used to constrain the spectral index assuming the γ rays produced by the π^0's accompanying the $\pi^{\pm}$'s escape the source. In such a scenario, Fig. 7 shows that only a relatively hard extragalactic spectrum is consistent with the data. On the other hand, the Galactic photon flux in the 10 GeV region is about an order of magnitude larger than than the extragalactic flux; this allows easier accommodation of a softer single power law spectrum. For the Galactic hypothesis, however, one must consider an important caveat, namely that the expected photon flux in the PeV range has been elusive [78]. However, a recent refined analysis of archival data from the EAS-MSU experiment [79] has confirmed previous claims of photons in the 10 PeV region. This analysis also results in a larger systematic uncertainty at all energies, relaxing previously reported bounds in the PeV range. While previous bounds were marginally consistent with nonobservation of PeV photons expected to accompany the IceCube neutrinos [20], this new less stringent bound is more comfortably consistent.

There is an additional interesting consequence of the new IceCube data. The neutrino spectral index should follow the source spectrum of the parent cosmic rays. We have shown elsewhere [20,80] that a spectral index of ~ 2.4 is required for consistency with current bounds on cosmic ray anisotropy. Further credence regarding our best-fit spectral index has been recently developed via numerical simulations [81]. It is worth stressing that our discussion regarding source energetics assumes the canonical Fermi index of $\alpha = 2$. Given the current level of uncertainties on the atmospheric neutrino background, the spatial distribution and total number of microquasars, as well as the large

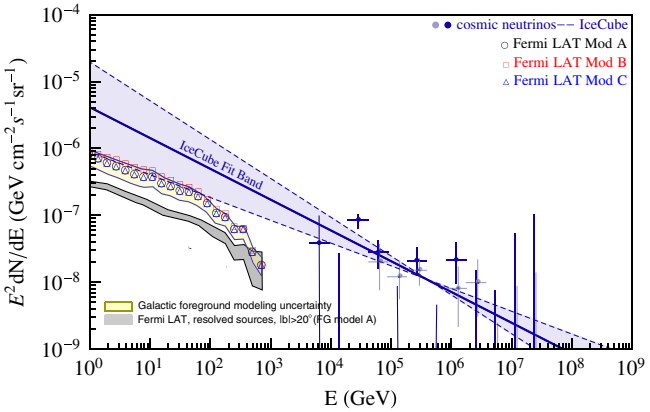

FIG. 7 (color online). The open symbols represent the total extragalactic γ-ray background for different foreground (FG) models as reported by the Fermi Collaboration [77]. For details on the modeling of the diffuse Galactic foreground emission in the benchmark FG models A, B, and C, see Ref. [77]. The cumulative intensity from resolved Fermi LAT sources at latitudes $|b| > 20°$ is indicated by a (gray) band. The solid symbols indicate the neutrino flux reported by the IceCube Collaboration. The best fit to the data (extrapolated down to lower energies), $\Phi(E_\nu) = 2.06^{+0.4}_{-0.3} \times 10^{-18}(E_\nu/10^5\ \mathrm{GeV})^{-2.46\pm0.12}\ \mathrm{GeV}^{-1}\ \mathrm{cm}^{-2}\ \mathrm{s}^{-1}\ \mathrm{sr}^{-1}$, is also shown for comparison.

variation in microquasar jet luminosities (see Table I), shifting our assumed spectral index from $\alpha = 2$ to $\alpha = 2.4$ will have little impact on the arguments concerning energetics explored herein. In the future, improved measurements all around will require a considerably more elaborate analysis, including detailed numerical simulations.

VI. CONCLUSIONS

Motivated by recent IceCube observations, we have reexamined the idea that μQSOs are high-energy neutrino emitters. We considered the particular case of LS 5039, which as of today represents the source with lowest p-value in the IceCube sample of selected targets [1]. We have shown that if LS 5039 has a compact object powering jets, it could accelerate protons up to above about 30 PeV. These highly relativistic protons could subsequently interact with the plasma producing a neutrino beam that could reach the maximum observed energies, $E_\nu \gtrsim$ PeV. There are two extreme possibilities for neutrino production: (i) close to the base of the jet and (ii) at the termination point of the jet. By normalizing the accompanying photon flux to H.E.S.S. observations in the TeV energy range [36,37], we have shown that, for the first scenario, photon absorption on the radiation field leads to a neutrino flux $\mathcal{O}(10^{-8}E_\nu^{-2}$ $\mathrm{GeV}^{-1}\ \mathrm{cm}^{-2}\ \mathrm{s}^{-1})$. Should this be the case, the neutrino flux almost saturates the current upper limit reported by the ANTARES Collaboration [53]. The second possibility yields a flux of neutrinos which is about an order of magnitude smaller. *A priori* these two extreme flux predictions are partially consistent with existing data.

[3]Evaluating the background, of course, requires detailed knowledge of detector properties and properly belongs to the territory of the IceCube Collaboration.

However, one can ask why a source with similar characteristics (LS I + 61 303) which is in the peak of the field of view of IceCube has not been already discovered. The current 90% C.L. upper limit on LS I + 61 303 reported by the IceCube Collaboration is $\mathcal{O}(10^{-9} E_\nu^{-2}\,\mathrm{GeV}^{-1}\,\mathrm{cm}^{-2}\,\mathrm{s}^{-1})$, favoring neutrino production near the end of LS 5039 jets.

We have also generalized our discussion to the population of μQSOs in the Galaxy. Using the spatial density distribution of high-mass x-ray binaries obtained from the deep INTEGRAL Galactic plane survey and assuming LS 5039 typifies the μQSO population, we have demonstrated that these powerful compact sources could provide the dominant contribution to the diffuse cosmic neutrino flux. Of course, a complete picture which accommodates all the shower events outside the Galactic plane may well require an extragalactic component. Indeed most of the istropic background is dominated by muon tracks. Explaining the possible isotropy of shower events may eventually prove only to be possible by considering extragalactic sources. Future IceCube observations will test the LS 5039 hypothesis, providing the final verdict for the ideas discussed in this paper.

ACKNOWLEDGMENTS

This work was supported in part by the US NSF Grants No. CAREER PHY-1053663 (L. A. A., L. H. M. da S.), No. PHY-1314774 (H. G.), and No. PHY-1205854 (T. C. P.); the NASA Grants No. NNX13AH52G (L. A. A., T. C. P.), No. AYA-ESP2012-39115-C03, No. AYA-ESP2013-47816-C4, and No. MULTIDARK Consolider CSD2009-00064 (B. J. V.). L. A. A. and T. C. P. thank the Center for Cosmology and Particle Physics at New York University for their hospitality.

[1] M. G. Aartsen *et al.* (IceCube Collaboration), Phys. Rev. Lett. **111**, 021103 (2013); Science **342**, 1242856 (2013); Phys. Rev. Lett. **113**, 101101 (2014).
[2] S. L. Glashow, Phys. Rev. **118**, 316 (1960).
[3] L. A. Anchordoqui, H. Goldberg, F. Halzen, and T. J. Weiler, Phys. Lett. B **621**, 18 (2005).
[4] G. J. Feldman and R. D. Cousins, Phys. Rev. D **57**, 3873 (1998).
[5] V. Barger, L. Fu, J. G. Learned, D. Marfatia, S. Pakvasa, and T. J. Weiler, arXiv:1407.3255.
[6] J. Abraham *et al.* (Pierre Auger Collaboration), Phys. Lett. B **685**, 239 (2010).
[7] L. A. Anchordoqui *et al.*, arXiv:1307.5312.
[8] For exotic explanations see e.g.,L. A. Anchordoqui, V. Barger, H. Goldberg, J. G. Learned, D. Marfatia, S. Pakvasa, T. C. Paul, and T. J. Weiler, Phys. Lett. B **739**, 99 (2014); K. C. Y. Ng and J. F. Beacom, Phys. Rev. D **90**, 065035 (2014); F. W. Stecker and S. T. Scully, Phys. Rev. D **90**, 043012 (2014); J. G. Learned and T. J. Weiler, arXiv:1407.0739.
[9] K. Murase, M. Ahlers, and B. C. Lacki, Phys. Rev. D **88**, 121301 (2013); I. Tamborra, S. 'i. Ando, and K. Murase, J. Cosmol. Astropart. Phys. 09 (2014) 043.
[10] L. A. Anchordoqui, V. Barger, I. Cholis, H. Goldberg, D. Hooper, A. Kusenko, J. G. Learned, D. Marfatia, S. Pakvasa, T. C. Paul, and T J. Weiler, J. High Energy Astrophys. **1–2**, 1 (2014).
[11] L. A. Anchordoqui, H. Goldberg, F. Halzen, and T. J. Weiler, Phys. Lett. B **600**, 202 (2004).
[12] A. Loeb and E. Waxman, J. Cosmol. Astropart. Phys. 05 (2006) 003.
[13] L. A. Anchordoqui, T. C. Paul, L. H. M. da Silva, D. F. Torres, and B. J. Vlcek, Phys. Rev. D **89**, 127304 (2014); J. B. Tjus, B. Eichmann, F. Halzen, A. Kheirandish, and S. M. Saba, Phys. Rev. D **89**, 12, 123005 (2014).
[14] E. Waxman and J. N. Bahcall, Phys. Rev. Lett. **78**, 2292 (1997); K. Murase, K. Ioka, S. Nagataki, and T. Nakamura, Astrophys. J. **651**, L5 (2006); I. Cholis and D. Hooper, J. Cosmol. Astropart. Phys. 06 (2013) 030.
[15] K. Murase, S. Inoue, and S. Nagataki, Astrophys. J. **689**, L105 (2008).
[16] F. Zandanel, I. Tamborra, S. Gabici, and S. Ando, arXiv:1410.8697.
[17] O. E. Kalashev, A. Kusenko, and W. Essey, Phys. Rev. Lett. **111**, 4, 041103 (2013); F. W. Stecker, Phys. Rev. D **88**, 4, 047301 (2013); P. Padovani and E. Resconi, Mon. Not. R. Astron. Soc. **443**, 474 (2014); S. S. Kimura, K. Murase, and K. Toma, arXiv:1411.3588.
[18] M. Ahlers and F. Halzen, Phys. Rev. D **90**, 043005 (2014).
[19] D. B. Fox, K. Kashiyama, and P. Mészarós, Astrophys. J. **774**, 74 (2013); A. Neronov, D. V. Semikoz, and C. Tchernin, Phys. Rev. D **89**, 103002 (2014).
[20] L. A. Anchordoqui, H. Goldberg, M. H. Lynch, A. V. Olinto, T. C. Paul, and T. J. Weiler, Phys. Rev. D **89**, 083003 (2014).
[21] S. Razzaque, Phys. Rev. D **88**, 081302 (2013).
[22] Y. Bai, A. J. Barger, V. Barger, R. Lu, A. D. Peterson, and J. Salvado, Phys. Rev. D **90**, 063012 (2014).
[23] J. Braun, J. Dumm, F. De Palma, C. Finley, A. Karle, and T. Montaruli, Astropart. Phys. **29**, 299 (2008).
[24] F. A. Aharonian, L. A. Anchordoqui, D. Khangulyan, and T. Montaruli, J. Phys. Conf. Ser. **39**, 408 (2006).
[25] I. F. Mirabel and L. F. Rodriguez, Nature (London) **371**, 46 (1994).
[26] I. F. Mirabel and L. F. Rodriguez, Annu. Rev. Astron. Astrophys. **37**, 409 (1999).
[27] A. A. Lutovinov, M. G. Revnivtsev, S. S. Tsygankov, and R. A. Krivonos, Mon. Not. R. Astron. Soc. **431**, 327 (2013).
[28] H. J. Grimm, M. Gilfanov, and R. Sunyaev, Astron. Astrophys. **391**, 923 (2002).
[29] J. S. Clark, P. Reig, S. P. Goodwin, L. M. Larionov, P. Blay, M. J. Coe, J. Fabregat, I. Negueruela, I. Papadakis, and I. A. Sttele, Astron. Astrophys. **376**, 476 (2001).

[30] M. V. McSwain, D. R. Gies, W. Huang, P. J. Wiita, D. W. Wingert, and L. Kaper, Astrophys. J. **600**, 927 (2004).
[31] J. Casares, M. Ribo, I. Ribas, J. M. Paredes, J. Marti, and A. Herrero, Mon. Not. R. Astron. Soc. **364**, 899 (2005).
[32] C. Aragona, M. V. McSwain, E. D. Grundstrom, A. N. Marsh, R. M. Roettenbacher, K. M. Hessler, T. S. Boyajian, and P. S. Ray, Astrophys. J. **698**, 514 (2009).
[33] G. E. Sarty *et al.*, Mon. Not. R. Astron. Soc. **411**, 1293 (2011).
[34] J. Moldon, M. Ribo, J. M. Paredes, W. Brisken, V. Dhawan, M. Kramer, A. G. Lyne, and B. W. Stappers, arXiv: 1205.2080.
[35] A. A. Abdo *et al.* (Fermi LAT Collaboration), Astrophys. J. **706**, L56 (2009).
[36] F. Aharonian *et al.* (H.E.S.S. Collaboration), Science **309**, 746 (2005).
[37] F. Aharonian *et al.* (H.E.S.S. Collaboration), Astron. Astrophys. **460**, 743 (2006).
[38] J. M. Paredes, J. Marti, M. Ribo, and M. Massi, Science **288**, 2340 (2000).
[39] J. M. Paredes, M. Ribo, E. Ros, J. Marti, and M. Massi, Astron. Astrophys. **393**, L99 (2002).
[40] M. Ribo, J. M. Paredes, J. Moldon, J. Marti, and M. Massi, Astron. Astrophys. **481**, 17 (2008).
[41] G. Dubus, Astron. Astrophys. **456**, 801 (2006).
[42] A. Sierpowska-Bartosik and D. F. Torres, Astrophys. J. **674**, L89 (2008).
[43] A. Sierpowska-Bartosik and D. F. Torres, Astropart. Phys. **30**, 239 (2008).
[44] M. V. McSwain, P. S. Ray, S. M. Ransom, M. S. E. Roberts, S. M. Dougherty, and G. G. Pooley, Astrophys. J. **738**, 105 (2011).
[45] N. Rea, D. F. Torres, G. A. Caliandro, D. Hadasch, M. van der Klis, P. G. Jonker, M. Mendez, and A. Sierpowska-Bartosik, Mon. Not. R. Astron. Soc. **416**, 1514 (2011).
[46] A. Levinson and E. Waxman, Phys. Rev. Lett. **87**, 171101 (2001).
[47] G. M. Frichter, T. K. Gaisser, and T. Stanev, Phys. Rev. D **56**, 3135 (1997).
[48] M. Bottcher and C. D. Dermer, Astrophys. J. **634**, L81 (2005).
[49] F. A. Aharonian and A. V. Plyasheshnikov, Astropart. Phys. **19**, 525 (2003).
[50] D. Khangulyan and F. Aharonian, AIP Conf. Proc. **745**, 359 (2005).
[51] R. C. Hartman *et al.* (EGRET Collaboration), Astrophys. J. Suppl. Ser. **123**, 79 (1999).
[52] C. Distefano, D. Guetta, E. Waxman, and A. Levinson, Astrophys. J. **575**, 378 (2002).
[53] S. Adrian-Martinez *et al.* (ANTARES Collaboration), Astrophys. J. **786**, L5 (2014).
[54] Q. Z. Liu, J. van Paradijs, and E. P. J. v. d. Heuvel, Astron. Astrophys. **455**, 1165 (2006).
[55] Q. Z. Liu, J. van Paradijs, and E. P. J. v. d. Heuvel, Astron. Astrophys. **469**, 807 (2007).
[56] R. Krivonos, S. Tsygankov, A. Lutovinov, M. Revnivtsev, E. Churazov, and R. Sunyaev, Astron. Astrophys. **545**, A27 (2012).
[57] J. M. Paredes and J. M. Marti, Contributions to Science **2**, 303 (2003), Institut d'Estudis Catalans, Barcelona.
[58] M. Massi, M. Ribó, J. Paredes, M. Peracaula, and R. Estalella, Astron. Astrophys. **376**, 217 (2001).
[59] A. A. Zdziarski, M. Gierlinski, J. Mikolajewska, G. Wardzinski, B. A. Harmon, and S. Kitamoto, Mon. Not. R. Astron. Soc. **351**, 791 (2004).
[60] V. Bosch-Ramon, G. E. Romero, J. M. Paredes, A. Bazzano, M. Del Santo, and L. Bassani, Astron. Astrophys. **457**, 1011 (2006).
[61] R. Soria, J. W. Broderick, J. Hao, D. C. Hannikainen, M. Mehdipour, K. Pottschmidt, and S. N. Zhang, arXiv: 1103.3009.
[62] D. M. Russell, R. P. Fender, E. Gallo, and C. R. Kaiser, Mon. Not. R. Astron. Soc. **376**, 1341 (2007).
[63] I. F. Mirabel, V. Dhawan, R. P. Mignani, I. Rodrigues, and F. Guglielmetti, Nature (London) **413**, 139 (2001).
[64] I. F. Mirabel and I. Rodrigues, Astron. Astrophys. **398**, L25 (2003).
[65] M. G. Aartsen *et al.* (IceCube Collaboration), Phys. Rev. D **87**, 6, 062002 (2013).
[66] M. Ahlers and K. Murase, Phys. Rev. D **90**, 023010 (2014).
[67] J. Albert *et al.* (MAGIC Collaboration), Science **312**, 1771 (2006); V. A. Acciari *et al.*, arXiv:0802.2363; A. A. Abdo *et al.* (Fermi LAT Collaboration), Astrophys. J. **701**, L123 (2009); D. Hadasch *et al.*, Astrophys. J. **749**, 54 (2012).
[68] M. Massi, M. Ribo, J. M. Paredes, S. T. Garrington, M. Peracaula, and J. Marti, Astron. Astrophys. **414**, L1 (2004).
[69] W. Bednarek, Mon. Not. R. Astron. Soc. **397**, 1420 (2009); D. F. Torres, N. Rea, P. Esposito, J. Li, Y. Chen, and S. Zhang, Astrophys. J. **744**, 106 (2012).
[70] D. F. Torres and F. Halzen, Astropart. Phys. **27**, 500 (2007).
[71] M. Ackermann *et al.* (AMANDA Collaboration), Phys. Rev. D **71**, 077102 (2005); A. Achterberg *et al.* (IceCube Collaboration), Phys. Rev. D **75**, 102001 (2007); R. Abbasi *et al.* (IceCube Collaboration), Phys. Rev. D **79**, 062001 (2009); R. Abbasi *et al.* (IceCube Collaboration), Astrophys. J. **701**, L47 (2009).
[72] M. G. Aartsen *et al.* (IceCube Collaboration), arXiv: 1406.6757.
[73] S. Adrian-Martinez *et al.* (ANTARES Collaboration), Journal of High Energy Astrophysics **3–4**, 9 (2014).
[74] T. K. Gaisser, F. Halzen, and T. Stanev, Phys. Rep. **258**, 173 (1995); **271**, 355(E) (1996).
[75] W. Dehnen and J. Binney, Mon. Not. R. Astron. Soc. **294**, 429 (1998).
[76] M. G. Aartsen *et al.* (IceCube Collaboration), arXiv: 1410.1749.
[77] M. Ackermann *et al.* (Fermi LAT Collaboration), arXiv: 1410.3696.
[78] A. Borione *et al.*, Astrophys. J. **493**, 175 (1998); M. C. Chantell *et al.* (CASA-MIA Collaboration), Phys. Rev. Lett. **79**, 1805 (1997).
[79] Y. A. Fomin, N. N. Kalmykov, G. V. Kulikov, V. P. Sulakov, and S. V. Troitsky, arXiv:1410.2599.
[80] L. A. Anchordoqui, H. Goldberg, A. V. Olinto, T. C. Paul, B. J. Vlcek, and T. J. Weiler, J. Phys. Conf. Ser. **531**, 012009 (2014).
[81] G. Giacinti, M. Kachelriess, and D. V. Semikoz, Phys. Rev. D **90**, 041302 (2014).